

## NMR Methods for the Fast Recording of Diffusion

Guilhem Pages,<sup>1</sup> Philip W. Kuchel,<sup>1</sup>

<sup>1</sup> University of Sydney, School of Molecular and Microbial Biosciences, Sydney 2006, Australia

Corresponding author:  
Guilhem Pages  
School of Molecular and Microbial Biosciences  
University of Sydney  
NSW 2006, Australia  
E-Mail: g.pages@mmb.usyd.edu.au

### Abstract

The time taken to complete an NMR diffusion experiment is typically ~10 minutes. For systems that rapidly evolve conventional pulsed field gradient spin-echo (PGSE) experiments cannot be used to obtain reliable estimates of molecular mobility. Modern 'fast-diffusion' experiments provide a means of obtaining this information and thus open up new vistas for the application of PGSE NMR. In this paper we review the various advantages and disadvantages of these methods.

**Keywords:** Diffusion experiment; diffusion ordered spectroscopy; DOSY; echo train; fast diffusion; lineshape fitting; multiple coherence pathways; single scan.

**Abbreviations:** BPPSTE, bipolar stimulated echo; CPMG, Carr-Purcell-Meiboom-Gill; DDF, distant dipolar field; DOSY, diffusion ordered spectroscopy; FID, free induction decay; MMME, multiple modulation multiple echoes; NMR, nuclear magnetic resonance; PFG, pulsed field gradient; PFGMSE, pulsed-field gradient multiple spin-echo; S/N, signal to noise ratio.

### 1. Introduction

Pulsed field gradient spin-echo nuclear magnetic resonance (PGSE NMR) experiments are a method of choice for studying diffusional mobility of molecules in living and inanimate systems. The method is non-invasive and is able to measure in a few minutes the diffusion coefficients of solutes and solvents in complex mixtures [1-5]. In PGSE NMR the signal intensity  $S(g)$  of the molecule of interest is measured as a function of the magnitude of the magnetic field gradient pulses that are used. The diffusion coefficient  $D$  is estimated from the data by regressing onto them the following Stejskal-Tanner equation [6]:

$$S(g) = S_0 e^{-\gamma^2 g^2 \delta^2 D \Delta} \quad (1)$$

where  $S_0$  denotes the signal intensity without gradients,  $\gamma$  is the nuclear magnetogyric ratio,  $g$  is the gradient amplitude,  $\delta$  is the gradient pulse duration, and  $\Delta'$  is the 'corrected' diffusion time. In the simplest pulse sequences  $\Delta'$  is simply the interval between the two field gradient pulses, or more generally  $\Delta' = (\Delta - \delta/3)$ .

One well-known extension to data acquisition and processing using PGSE NMR is diffusion ordered spectroscopy (DOSY) [7]. The final output is a 2-dimensional contour map in which one axis records diffusion coefficients and the other chemical shifts. Thus one dimension indicates a physical property and not, as is usually the case, information on magnetic interactions between nuclei.

New pulse sequences and processing methods have been developed to study a diverse variety of samples from: discrete to polydisperse samples; chemical to biological ones; unrestricted to restricted ones or those with anisotropic diffusion; and stagnant to rapidly flowing mixtures. Several reviews have been written describing these applications [1,3,8-10].

Even if the total time of the experiment is short, it may be too long to interrogate systems in which diffusion coefficients change rapidly. Such systems include biological ones with enzyme-catalyzed reactions, or those in rapidly flowing fluids in industrial processes. The first fast-diffusion NMR pulse sequence was described in 1969 [11]; and recently a few more methods have been published that can measure a diffusion coefficient in less than 1 minute. We review these techniques in this paper.

Pulse sequences to measure diffusion coefficients very rapidly have also been developed to handle the specific requirements of grossly inhomogeneous magnetic fields [12], and for use with laser-excited hyper-polarized gas of relatively short half-life [13]. Because these methods are highly specialized we will not discuss with them in any detail. We have classified the remainder of the methods into two classes: (1) those from which the diffusion coefficient is extracted from data obtained by using only one or two gradient pulses; and (2) those in which diffusion is elicited by a train of gradient pulses. The latter we analyze and discuss first.

## 2. Diffusion measured using a train of gradient pulses

### *Saving time by decreasing phase cycling*

By keeping to the traditional approach with PGSE NMR experiments the only recourse to saving time is to decrease the number of transients in each phase cycle. In the bipolar-pulse stimulated-echo (BPPSTE) experiment [14], the phase cycling of the  $180^\circ$  pulses requires a EXORCYCLE [15] with 16 (or optimally 64) transients in order to record only the spatially encoded magnetization. This EXORCYCLE enforces a zero-order coherence during the delay  $\Delta$ .

The approach developed by Morris et al. [16] is based on suppression of unwanted coherence-transfer pathways using deliberately unbalanced pulse pairs (Fig. 1). The magnitude of the two pulses in a pair have the ratio  $1:1+\alpha$ . During the experiment,  $\alpha$  is held constant and the appropriately transformed Stejskal-Tanner equation is:

$$\frac{S(g)}{S(0)} = e^{-\gamma^2 g^2 \delta^2 (\Delta + \delta \frac{\alpha^2 - 2}{6} + \tau \frac{\alpha^2 - 1}{2})} \quad (2)$$

where  $\tau$  denotes the delay between the two components of the bipolar magnetic field gradient pulses. The choice of the value of  $\alpha$  depends on  $B_1$  inhomogeneity and signal-to-noise ratio and is usually  $\sim 0.2$ .

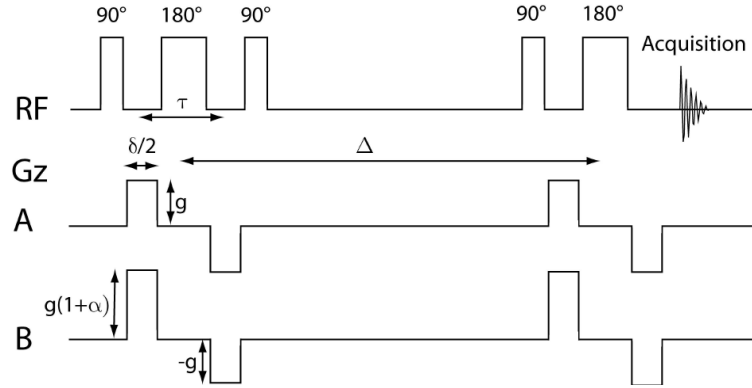


**Fig. 1:** PGSE pulse sequences that use composite pulses. **A**, classical BPPLIED sequence **B**, the pulse sequence designed by Morris et al. [16] that uses unequal gradient pulses in each bipolar pair. Additional gradient pulses can be used in **B** to refocus the lock signal and to dephase unwanted coherences. Spoil gradients can also be added to the BPPLIED pulse sequence. RF denotes the radio-frequency time train and Gz the gradient pulse time train.  $\delta$  is the gradient duration,  $g$  is the gradient amplitude,  $\Delta$  is the diffusion time (midpoints of the two diffusion encoding periods),  $\tau$  is the time between the midpoints of the antiphase field gradients, and  $\alpha$  is the unbalancing factor of the gradient pulses.

### *Series of gradient echoes*

Another way to minimize the acquisition time of a PGSE experiment is to record within a single transient the echoes that are modulated by diffusion. There are four pulse sequences that are based on this principle.

The first two pulse sequences are based on the Carr–Purcell–Meiboom–Gill (CPMG) experiment. In one, each 180° pulse is sandwiched between two gradient pulses of identical magnitude to encode and then decode spatial information (Fig. 2A); the pulse sequence is called the Pulsed Field-Gradient Multiple Spin-Echo (PFGMSE) experiment [17]. The delay between the initial 90° pulse and the first 180° is  $\tau$  and the delay between each 180° is twice this value,  $2\tau$ , and each echo corresponds to a different gradient magnitude. The number of echoes that are recorded is the number of points used in the diffusion decay analysis, so a prolonged series of echoes provides a better estimate of  $D$ . To extract the value of  $D$ , the ratios between two consecutive echoes must be calculated (Eq. 3). It is then a simple matter to determine  $D$  from the slope of the graph:

$$\ln \frac{S(n+1)}{S(n)} = -\frac{2\tau}{T_2} - \gamma^2 n^2 g^2 \delta^2 D \Delta' \quad (3)$$

where  $n$  denotes to the  $n$ th echo that is recorded.

The second pulse sequence, that is based on a CPMG RF-pulse train, uses magnetic field gradient pulses that are of constant amplitude (Fig. 2B) [18]. The diffusion coefficient is extracted from the linewidths of the Fourier transform of the echo train. The width of the resonance at half of the peak height,  $\Delta\nu_{1/2}$ , of the adsorption signal in the frequency domain, for a Lorentzian lineshape is:

$$\Delta\nu_{1/2} = \frac{1}{\pi} \left[ \frac{1}{T_2} + \gamma^2 g^2 \delta^2 D \left( \frac{\Delta}{2\tau} - \frac{\delta}{6\tau} \right) \right] \quad (4)$$

To fit the data, the value of the first term in parentheses of Eq. (4) is required. Hence an experiment is run with the gradient pulse-amplitudes set to 0 thus eliminating the second term of the equation.

To extend this method to the case of non-Lorentzian lineshapes and/or overlapping peaks in the echo spectrum, the first  $90^\circ$  hard pulse is substituted by a  $90^\circ$  selective one. Fig. 2 emphasizes the similarity between both of the CPMG-based pulse sequences. They differ only in the variation or not of the gradient magnitudes.

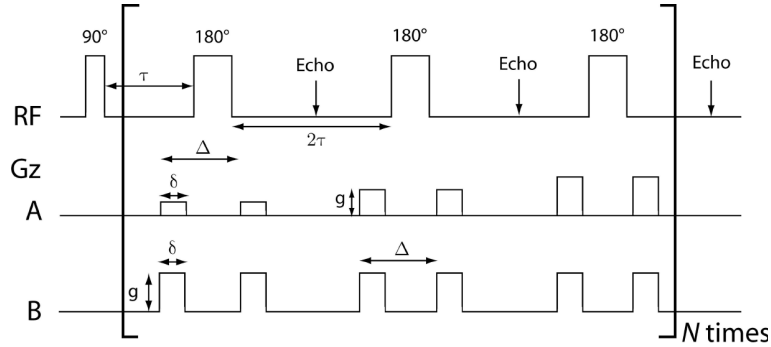


**Fig. 2:** CPMG-based PGSE methods for measuring  $D$  in a single multiple-echo transient. **A**, the PGMSE method [17]; and **B**, the method of Chandrakumar et al. [18]. For **A** the gradient amplitude is increased systematically, while for **B** it is constant. The notation is identical to that in Fig. 1 except that  $\tau$  is the delay between the  $90^\circ$  and  $180^\circ$  RF pulses. The subscripted square-brackets around the pulse sequence indicates that it is repeated  $N$  times.

The third method in the present class involves recording a series of echoes that are created by alternation of the diffusion gradient [19]; these are called gradient echoes. Each echo is attenuated further by an additional diffusion-gradient pulse. The expression for the signal amplitude differs between even (Eq. 5) and odd (Eq. 6) echoes:

$$S_{even-n} = A_n e^{-2\gamma^2 g^2 n \delta^3 \frac{D}{3}} e^{2\gamma^2 g_0 \cdot g n \delta^3 D} \quad (5)$$

$$S_{odd-n} = A_n e^{-2\gamma^2 g^2 n \delta^3 \frac{D}{3}} e^{2\gamma^2 \mathbf{g}_0 \cdot \mathbf{g} D (\tau \delta^2 - n \delta^3)} \quad (6)$$

where  $A_n$  is the amplitude without diffusion attenuation, and the vector dot product  $\mathbf{g}_0 \cdot \mathbf{g}$  accounts for the interaction between the gradient pulses and a static magnetic field. Fitting the signal amplitude using both previous equations is used to estimate  $D$ .

Finally, a recent approach called Difftrain has been described [20]. This is like the previous one because it exploits attenuation of an echo by an additional gradient pulse. The position of a nucleus is encoded and then it is decoded multiple times. This yields all the information necessary to fit the Stejskal-Tanner equation (Eq. 1). To conserve chemical shift information, the pulse sequence uses the inversion recovery method that is routinely used for measuring longitudinal relaxation times [21]. Positions of the spins are encoded in the transverse plane and then promoted to the longitudinal direction with an RF pulse; then a small proportion of the spin population is returned to the transverse plane for the detection via a spin echo. After detection, the residual magnetization is destroyed by a spoil gradient, before applying another gradient and RF pulse to detect the next echo.

Difftrain can be used to measure the distribution of droplet sizes in an oil-water emulsion that is undergoing evolution during phase separation [22]. A fast-diffusion experiment (taking less than 4 s) was needed to characterize the system because the emulsion was thermodynamically unstable. In contrast, the acquisition time for a classical PGSE NMR experiment is too long to capture the evolving droplet sizes in the system. The authors also describe the possibility of measuring the apparent velocity of water flow through an ion-exchange (desalting) column.

All the abovementioned experiments take significantly less time than the classical PGSE NMR diffusion experiments to yield their data. They are still based on the evolution of a signal whose variation is described by an expression that contains  $D$ . Comparing the methods, the one described by Morris et al. [16] appears to encompass the best compromise between the difficulty of setting up the experiment on the NMR spectrometer and processing the resulting data. Other approaches have been developed to measure  $D$  in a single-scan, but the major difference is that they do not require a change in gradient magnitude during the experiment.

### 3. Pulse sequences with a small number of gradients

#### *Burst pulse sequence*

The Burst pulse sequence [23], was initially developed to rapidly acquire magnetic resonance images (MRI) under conditions of high spectral resolution [24]. A train of echoes is created from a series of low flip-angle RF pulses. To enable image formation, the pulses are applied in the presence of a persistent magnetic field gradient; and the echoes are detected by using a magnetic ‘read’ gradient (Fig. 3).

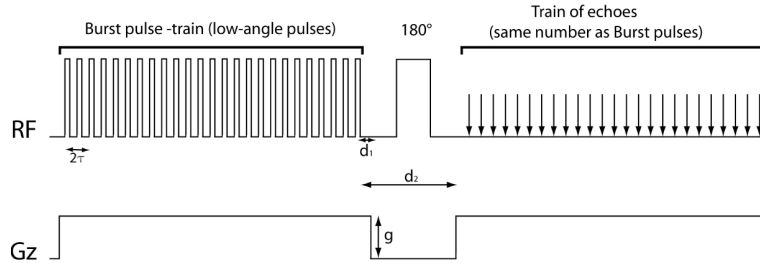


**Fig. 3:** The Burst pulse sequence modified to measure  $D$  [24]. On the upper right of the diagram each arrow represents an echo;  $d_1$  is the delay between the end of the last pulse and switching off the gradient;  $d_2$  is the period between the last RF pulse and switching the read gradient on;  $\tau$  is the period between the midpoints of two consecutive RF pulses. For other notation, see Fig. 1.

To analyze the effect of this pulse sequence on a spin system we note that the first series of RF pulses is simply a DANTE pulse train [25]. This realization suggests the use of the ‘small-angle approximation’ [26] that is used in predicting the excitation envelope of the pulse train. The analysis is then extended to include the effects of diffusion. Accordingly the signal intensity for each echo is described by the equation:

$$S_n = e^{-\gamma^2 g^2 \delta_n^2 D \left( \Delta_n - \frac{\delta_n}{3} \right)} \quad (7)$$

where  $\Delta_n = n\tau + d_2$  and  $\delta_n = n\tau + d_1$ .  $D$  is estimated by fitting Eq. (7) to a graph of the intensity of the NMR signal versus the grouped parameters in the exponent of the expression.

#### **Multiple Modulation Multiple Echoes (MMME)**

A further method to rapidly estimate  $D$  of a molecular species is to record the spin-echo from a series of different coherence pathways. This approach increases the information content over that of a single-transient [27]. For spin-1/2 nuclei such as  $^1\text{H}$ , we can define three states of magnetization:  $M_0$ ,  $M_-$  and  $M_+$ . For a train of RF pulses, a coherence pathway is characterized by a series of  $N + 1$  numbers from  $q_0$  to  $q_N$  where  $q_N$  is the magnetization after the  $N^{\text{th}}$  pulse and  $q_0$  is the magnetization-state before the first pulse. Each coherence pathway can be written as a product of three terms:

$$M_Q = A_Q B_Q C_Q \quad (8)$$

where  $Q$  represents one coherence pathway between 0 and  $N$ ;  $A_Q$  is the frequency spectrum;  $B_Q$  is a term that describes diffusion; and  $C_Q$  is the relaxation-attenuation factor. To write an expression for  $B_Q$ , it is necessary to introduce the instantaneous wave-vector  $k(t)$  [28,29], the magnitude of the constant field-gradient  $g$  and the instantaneous value of  $q$ ,  $q(t)$ :

$$k(t) = \gamma g \int_0^t q(t') dt' \quad (9)$$

In the case of diffusion in an isotropic unbounded medium the attenuation of the signal is given by,

$$\mathbf{B}_Q = e^{-D \int_0^t k(t')^2 dt'} \quad (10)$$

where  $t = 0$  specifies the beginning of the pulse sequence and  $T$  is the time at the maximum of the spin echo.

Now consider a persistent magnetic field gradient and a train of four RF pulses with tipping angles  $\alpha_1, \dots, \alpha_4$  and a time spacing between them of  $\tau_1$  to  $\tau_3$ , respectively. Fig. 4 shows this sequence using  $\alpha_1 = \alpha_2 = \alpha_3 = 90^\circ$  and  $\alpha_4 = 180^\circ$ .

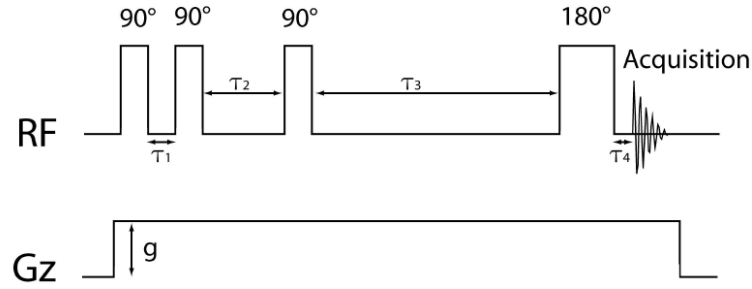


**Fig. 4:** MMME4 pulse sequence [27] used to measure  $D$  in a single transient. RF, Gz and  $g$  are defined in Fig. 1.  $\tau_1$  is chosen and then  $\tau_2$  and  $\tau_3$  are calculated using Eq. (15).

During the  $\tau$  periods in the pulse sequence of Fig. 4, transverse magnetization ( $q = \pm 1$ ) acquires a phase of  $qg\tau_i$  ( $i = 1, 2$  or  $3$ ) and the spin echo appears when the total phase is zero:

$$q_1\tau_1 + q_2\tau_2 + q_3\tau_3 - \tau_4 = 0 \quad (11)$$

where  $\tau_4$  is the delay after the last pulse and prior to acquisition of the free induction decay. For a ratio  $\tau_1 = \tau_2/3 = \tau_3/9$ , Eq. 11 is expressed by the ratio  $\tau_4/\tau_1$  which represents the phase index:

$$\tau_4/\tau_1 = q_1 + 3q_2 + 9q_3 \quad (12)$$

Therefore, fourteen different phase indices are obtained, and by using the convention,  $q_0 = 0$  and  $q_4 = -1$  to detect the signal it is seen that an echo is detected every  $\tau_4 = n\tau_1$

where  $n$  is the phase index. Thus we detect a new spin-echo signal every  $\tau_1$  seconds as indicated in Table 1.

Table 1: Different coherence pathways in a MMME4 pulse sequence. One free induction decay (coherence pathway 0,0,0,0,-1) with 13 echoes are recorded.

Phase index	$q_0$	$q_1$	$q_2$	$q_3$	$q_4$
0	0	0	0	0	-1
1	0	1	0	0	-1
2	0	-1	1	0	-1
3	0	0	1	0	-1
4	0	1	1	0	-1
5	0	-1	-1	1	-1
6	0	0	-1	1	-1
7	0	1	-1	1	-1
8	0	-1	0	1	-1
9	0	0	0	1	-1
10	0	1	0	1	-1
11	0	-1	1	1	-1
12	0	0	1	1	-1
13	0	1	1	1	-1

For each coherence pathway, molecular diffusion is responsible for signal attenuation which is described by the expression:

$$\mathbf{B}_Q = e^{-b_Q D r^2 g \tau^3} \quad (13)$$

where  $b_Q$  is calculated for each coherence pathway. The  $\mathbf{C}_Q$  term contains the longitudinal and transverse relaxation times,  $T_1$  and  $T_2$ , respectively.

The previous experiment can be extended to a sequence of  $N$  pulses whereupon it is called MMMEN. For  $N$  pulses, the number of coherence pathways that are generated is given by [30]:

$$[3^{(N-1)} - 1]/2 + 1 \quad (14)$$

Table 2 shows the number of coherence pathways that are recorded as a function of the number of RF pulses.

Table 2: Number of coherence pathways recorded for a pulse sequence incorporating from 2 to 7 RF pulses [26].

Number of RF pulses	2	3	4	5	6	7
Number of coherence pathways	2	5	14	41	122	365

In order to record spin echoes at particular times we set the period  $\tau_i$  to be a power of 3:

$$\tau_i = 3^{i-1} \tau_1 \quad (15)$$

Because the experiment is performed with a field gradient that is on all the time, and the sample extends beyond the region of the RF coils, each pulse must be slice-selective so that off-resonance signals are avoided. Using these conditions, the spin-echo signals and line shapes are able to be rigorously defined. Thus a single-transient experiment is sufficient to measure  $D$ . If the sample size is not sufficiently large spin-echoes may not have uniquely determined shapes and/or areas. In this case, two transients must be acquired using two different  $\tau$  values ( $\tau$  and  $\tau'$ ); then the diffusion coefficient is obtained from the ratio of the intensities of both echoes, as follows:

$$\frac{S_Q(\tau)}{S_Q(\tau')} = e^{-b_Q D \gamma^2 g^2 (\tau^3 - \tau'^3)} \quad (16)$$

This method has been successfully implemented in the SMART imaging pulse sequence [31,32]. The pulse sequence [31] measures both  $D$  and  $T_2$ , and for unspecified reasons it requires a phase cycle of four transients. MMME has also been applied to measuring the velocity of flowing fluid in a single transient [33]. By adding magnetic field gradient pulses in multiple directions, it is possible to record a diffusion tensor that characterizes diffusion in all three directions of a Cartesian coordinate system [34]. Thus the values of  $D_{xx}$ ,  $D_{yy}$ , and  $D_{zz}$  can be deduced for each dimension in anisotropic media using a single-transient.

#### ***Fast-CRAZED***

In this experiment RF pulses are used to excite spin systems in the sample so that a dipolar magnetic field is transiently established. This so called ‘distant dipolar field’ (DDF) is then used to measure simultaneously both  $D$  and  $T_2$ . Thus the CRAZED pulse sequence led to fast-CRAZED [35] due to its ability to rapidly measure the NMR parameters [36] (Fig. 5).

In this pulse sequence only one gradient pulse is used. The DDF created by the modulated magnetization performs the role of field gradient pulses by refocussing dephased magnetization. To select intermolecular zero-quantum transitions mediated by the DDF, a two-step phase cycle is used with a transient recorded with a  $\beta$  RF pulse (Fig. 5) of  $45^\circ$  subtracted from one recorded with  $\beta = 135^\circ$ . A train of  $180^\circ$  pulses is used as a sandwich of  $90^\circ$ -  $180^\circ$ -  $90^\circ$  pulses [37] to minimize the loss of magnitude of the DDF. The first  $90^\circ$  RF pulse can be an adiabatic one thus selecting particular coherence pathways. The total time for an experiment using this sequence is  $\sim 10$  seconds; the slightly longer time than perhaps expected is due to the long train of  $90^\circ$ -  $180^\circ$ -  $90^\circ$  pulses.

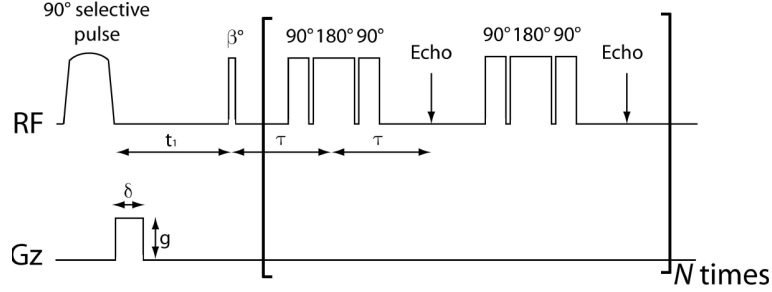


**Fig. 5:** Fast-CRAZED pulse sequence [38].  $\beta$  is a  $45^\circ$  or  $135^\circ$  RF pulse.  $t_1$  is the period between the end of the adiabatic pulse and the middle of the  $\beta$  pulse and  $\tau$  is the delay between the midpoints of the  $\beta$  pulse and the sandwiched  $180^\circ$  pulse. The sandwiched train is repeated  $N$  times. For other items of notation see Fig. 1.

The theoretical underpinning of this experiment relies on the non-linear term that is added to the Bloch-Torrey equations to account for the presence of the DDF [39-41]; the parameter  $D$  is incorporated into this term. An analytical solution of this equation is available only if diffusion-mediated signal-attenuation is much stronger than the rephasing of the magnetization due to the DDF. Thus diffusion attenuation is encapsulated in the relationship  $1/(D(\gamma g \delta)^2)$  while the dipolar characteristic time is given by:

$$\tau_d = \frac{1}{\mu_0 \gamma M_0} \quad (17)$$

where  $\mu_0$  is the magnetic permeability of a vacuum, and  $M_0$  is the equilibrium magnetization. The signal from the pulse sequence represented in Fig. 5 is given by Eq. (18) that includes the DDF in its local form [42] assuming that (see Fig. 5)  $t_1 \ll T_1$ .

$$\overline{M^+}(t_1, t_2) = \frac{M_0(3\cos^2\theta - 1)}{4\tau_d} \sin 2\beta e^{-2Dk^2(t_1 - \frac{2\delta}{3})} \times \frac{e^{-\frac{(2t_1+t_2)}{T_2}}}{2Dk^2 + \frac{1}{T_1}} \times (1 - e^{-(2Dk^2 + \frac{1}{T_1})t_2}) \quad (18)$$

where  $\theta$  is the angle between  $\mathbf{G}$  and  $\mathbf{B}_0$ , and  $\mathbf{k}$  is the wave vector of spatial modulation of the magnetization caused by the magnetic field gradient; it is equal to  $\gamma g \mathbf{G}$ . A log-normal plot of the signal amplitude versus  $t_2$  allows the extraction of estimates of both  $D$  and  $T_2$  as follows:

(i) if  $t_2 \gg \frac{1}{2Dk^2 + \frac{1}{T_1}}$ ,  $T_2$  is estimated from the slope of the function that is

fitted to the data.

(ii) if  $2Dk^2 \gg \frac{1}{T_1}$ ,  $D$  is obtained from the data by considering the value of  $T_1$  to

be effectively infinite and fitting the resulting expression.

### ***One-dimensional DOSY***

As noted above, a well-known data representation from PGSE NMR is called DOSY [7,9]; the experiment and subsequent data analysis generate a 2-dimensional contour map with the estimates of  $D$  along one axis and chemical shift along the other. In the realm of experiments used to rapidly measure  $D$  the name of a new method is derived from the fact that information on both diffusion and chemical shift are recorded using a single-transient; hence it is called one-dimensional DOSY [43,44].

The principle of the method is that information on diffusion is encoded in the lineshape of each resonance. To achieve this outcome there must be a spatial dependence of the chemical shift, and diffusion will broaden peaks during signal acquisition. There are two reported methods based on this principle that record data in a single transient, and from which the data are then analyzed to yield an estimate of  $D$ . The two methods differ in the way they create the spatial dependence of chemical shift. In the first method [43], this dependence is created by using a non-uniform magnetic field gradient that is generated by an additional current in the  $z^2$  shim coils, after a hardware modification that enables its switching on and off during the pulse sequence.

In the second method [44], spatial encoding is generated using an adiabatic frequency-swept  $180^\circ$  RF pulse that is applied while the diffusion-detecting magnetic field gradients are applied.

For both pulse sequences, the peak broadening that is invoked during signal acquisition is brought about with a weak linear ‘read’ gradient. But because the second method does not require hardware modification it is easier to implement than the first one. Therefore henceforth we focus on this pulse sequence (Fig. 6).

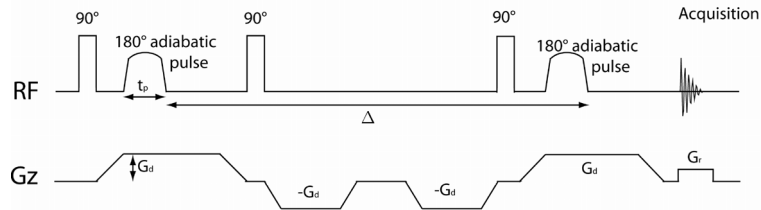


**Fig. 6:** One-dimensional DOSY pulse sequence [44]. Two negative gradient pulses are added to reduce eddy currents.  $t_p$  is the adiabatic pulse duration,  $G_d$  and  $G_r$  are, respectively, the intensity of the diffusion and read gradients, and  $\Delta$  is the diffusion time.

The diffusion gradients  $G_d$  are chosen to bring about different chemical shifts (off-set frequencies) as a function of spatial position. During the first of the magnetic field gradient pulses an adiabatic RF pulse of duration  $t_p$ , is swept through a range of off-set frequencies. The spins are nutated through the  $x',y'$ -plane by this pulse at different times during the application of the magnetic field gradient; thus they are exposed to diffusion sensing over different times depending on their spatial location in the sample. A schematic representation of this effect is shown in Fig. 7. For spins located at one end of the sample, the adiabatic RF  $180^\circ$  pulse exerts its effect immediately and their magnetization is dephased by the gradient field for a time  $t_p$ . On the other hand, magnetization in the middle of the sample is dephased during  $t_p/2$ , then the adiabatic swept-frequency RF  $180^\circ$  pulse is applied; finally the magnetization is dephased by the gradient pulse during the last  $t_p/2$  period. This last period leads to refocusing of the spin magnetization vectors. The combination of gradient and sweep pulse allows the acquisition of a net signal that depends on the spatial position of the spins. To record the signal attenuation along the sample, signal acquisition occurs in the presence of a read-gradient  $G_r$ . Therefore spectral peaks are obtained which are diffusion-weighted images of the sample, but the weighting varies along the sample.

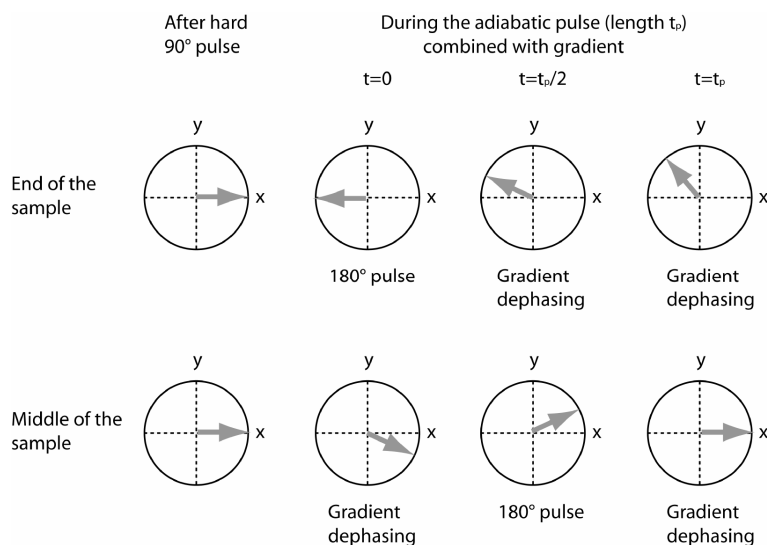


**Fig. 7:** One-dimensional DOSY. Effect of the first  $90^\circ$  hard pulse and then the adiabatic pulse and diffusion gradient, as a function of the position of spins (spin isochromats) in the sample. The time scale is that of the adiabatic RF pulse of duration  $t_p$ .

To analyze the data, the net phase acquired by spin isochromats at the end of the adiabatic pulse needs to be expressed as a function of the experimental parameters and  $D$ . Hence, if a spin at position  $z$  experiences RF-induced  $180^\circ$  flipping at time  $\alpha(z)t_p$ , where  $1 \geq \alpha(z) \geq 0$ , the following relationship holds:

$$\gamma G_d z \alpha(z) t_p - \gamma G_d z [1 - \alpha(z)] t_p = -[1 - 2\alpha(z)] \gamma G_d z t_p \quad (19)$$

During the frequency-sweep pulse, the spin isochromats precess as if they were under an effective gradient of strength  $G_{eff}$ :

$$G_{eff}(z) = [1 - 2\alpha(z)] G_d \quad (20)$$

In this simplified analysis it is assumed that the spin isochromats experience a  $180^\circ$  nutation at the instant the sweep is on-resonance. A more exact approach is described in the Appendix of the original paper [44].

After calculating the effective magnetic field gradient associated with each off-set frequency (chemical shift position, hence  $z$ ) a predicted lineshape is calculated for a value of  $D_{fit}$  using a slightly modified form of Eq. (1):

$$S(z) = S_0 e^{-\gamma^2 A_{eff}^2(z) D_{fit} \Delta} \quad (21)$$

where  $S_0$  is a scaling factor, and  $A_{eff}$  corresponds to  $G_{eff}(z) t_p$ .

#### 4. Limitations of fast-recording methods

##### *General*

None of the methods described above have been developed to estimate two different values of  $D$  from the one spectral peak. The systems that have been studied have been well defined ones, and applications to more complex heterogeneous samples are awaited. In the particular case of biological samples where the temperature is relatively high convection can introduce a systematic overestimate of the value of  $D$ , and yet none of the fast-diffusion methods are convection compensated [3,45]. In addition, the pulse sequences have not yet been used with systems that have restricted diffusion, such as water in red blood cells [46].

Another general limitation is the available signal-to-noise (S/N) ratio in the NMR spectra. The gain in time efficiency is off-set by a lower S/N ratio; only in systems in which the detection is facile, i.e., a high solute concentration, can the experiments be used.

The particular fast-diffusion methods that are based on the recording of spin-echoes [17-20,24,27,36] also have the same drawbacks related to S/N. To avoid the overlap of spin echoes, the intensity of each subsequent echo must be significantly less than the previous one. The second drawback is the loss of chemical shift information in these latter methods, making them inappropriate for studies on mixtures of solutes [18-20].

##### *Limitations of experiments with trains of gradients*

A common observation with respect to the estimates of  $D$ s obtained with fast-diffusion experiments is that they are high relative to those obtained with standard PGSE methods. The coefficient of variation on the estimates of  $D$  made from a peak that is

broad in the diffusion dimension of a 2-dimensional (DOSY) map, is routinely higher from a fast-diffusion pulse sequence. In the method of Morris et al. [16] errors arise from the presence of a small extra amount of signal that survives the pulse train due to an insufficient absolute difference in gradient area between the two last gradient pulses. This undesired residual signal increases the signal intensities above what is expected at the higher magnitudes of the field gradient pulses. This results in a smaller estimate of the apparent  $D$ . On the other hand, for the pulse sequences that use a CPMG RF-pulse train [17,18], an imperfect  $180^\circ$  refocusing pulse gives an error in the signal intensity that manifests itself as a faster decay and hence an artifactually high estimate of  $D$ .

For both of the CPMG-based methods, obviously the total acquisition time must be shorter than the  $T_2$  of the nuclei of interest. Unfortunately, in most cases, this condition can not be satisfied. The method of Van Gelderen et al. [19] allows the capture of chemical shift information when a large number of points are sampled in each gradient echo but the subsequent data processing is long and complex: both the chemical shift (off-set frequency) and gradient-induced evolution evolve in the opposite way. And, the data set from each echo must be processed separately.

In the CPMG methods the magnetic field gradient pulses must be switched on and off very rapidly, thus promoting eddy currents in conducting parts of the NMR probe. These give rise to distortion of spectral line shapes and lead to artifacts in the estimates of  $D$ .

The Difftrain pulse sequence has two drawbacks: The first is the requirement that the sample has long relaxation times, and there must be plenty of samples with a high S/N. The second, is the need to acquire two transients to estimate  $D$ : the first transient is recorded without the magnetic field gradient on to record the signal decay due to  $T_1$ ; while the second one is recorded with gradients to measure both diffusion and relaxation effects.

#### ***Limited gradient pulse methods***

The estimates of  $D$  obtained with the one-dimensional DOSY methods are often lower than those estimated with the more conventional PGSE methods. In performing the experiments the spectroscopist should have this consideration in mind. In order to have a coefficient of variation in the estimate of  $D$  of  $\sim 1.5\%$ , the S/N ratio should be greater than  $\sim 100$ . Because the CPMG-diffusion methods are based on analyzing diffusion-broadened spectral peaks, the likelihood of peak-overlap is increased; therefore fitting of the requisite lineshape function to the data can be problematical. To apply the methods to estimate the  $D$  of solutes in mixtures requires well-resolved peaks as a precondition.

For both the MMME and Burst pulse sequences, a long period is used for the evolution of the magnetization of the system, and this occurs in the presence of magnetic field gradients. This is especially true of MMME (Fig. 4) in which the gradients are on for the full duration of the pulse sequence. Even if the gradient magnitudes are only a few gauss per centimeter, the total experimental time is critical. The manufacturers recommend using gradient pulses that are on for less than 10 ms at the maximum current. If we consider a linear relationship between current and  $g$ , the maximum experimental time obtained by using only 1% of the maximum current is 1 second. Hence, this duration determines the maximum duration of the MMME pulse sequence.

The final inconvenience lies in the restricted domain of parameter values in which the equation that is used for estimating  $D$  from the data remains valid. For the Fast-CRAZED method, Eq. (18) is valid only in regimes of highly diffusion-attenuated signals. This is generally found in systems that contain small molecules in solution or in the gas phase. Furthermore, the number of transients that are needed to retrieve the parameters to fit with Eq. (18) increases with the number of components. Thus it appears that fast-diffusion experiments have only been applied, at most, with binary mixtures with each component being 'non dilute'. And with the Burst pulse sequence the total DANTE angle is made less than  $30^\circ$  to improve the veracity of the estimate of  $D$ . With the latter, and indeed all the pulse sequences discussed here, a significant amount of effort must be expended on trial experiments that are used to optimize performance on each particular NMR spectrometer.

## 5. Conclusions

A knowledge of the diffusion coefficients of solvent and solutes in mixtures of various origins is valuable for predicting the physical and chemically-reactive properties of the system. If systems of interest evolve rapidly on the time scale of conventional PGSE NMR diffusion experiments then the pulse sequences described here might be of value.

There are principally two different classes of NMR fast-diffusion experiments. The first records the signal as a function of the magnitude of the magnetic field gradients that are used in the experiment. To speed up signal acquisition various pulse sequences have been designed to minimize the extent of phase cycling; or to record a series of spin-echo signals from a range of magnitudes of the magnetic field gradients.

The second class of experiments uses only one or two magnetic field gradient magnitudes. To estimate  $D$ , spatial information is encoded by using a different approach from that commonly used in, say, the Stejskal-Tanner experiment [6]. Each method is based on a different physical phenomenon. The first uses a DANTE RF-pulse train, while the second pulse sequence achieves in one transient the sampling of many different magnetization-coherence pathways. The third method uses a distant dipolar field (DDF) and both adiabatic and gradient pulses are combined to give spectra from which  $D$  is estimated.

Each of the methods described presents its own limitations. None of the pulse sequences have been used to study restricted diffusion for which long diffusion times are usually needed. Systems in which there is convection pose another problem, as none of the methods are convection compensated.

Some of the methods record a train of spin-echoes, and chemical shift information is lost or is barely accessible, thus limiting the application of the methods to only simple mixtures of solutes.

Overall the one-dimensional DOSY method appears to be the method of choice for the (biological) systems which we study [3]. Currently, this method is being developed in our laboratory to study rapidly evolving systems such as the morphological changes in the human red blood cell, its membrane flickering, and the variation of  $D$  of guest molecules inside an extended support such as gelatin that undergoes changes in length [47,48].

## Acknowledgements

The work was supported by a Discovery Grant from the Australian Research Council to PWK.

## References

- [1] A.R. Waldeck, P.W. Kuchel, A.J. Lennon, B.E. Chapman, *Prog. Nucl. Magn. Reson. Spectrosc.* 30 (1997) 39-68.
- [2] K.I. Momot, P.W. Kuchel, *Concepts in Magnetic Resonance, Part A* 19A (2003) 51-64.
- [3] K.I. Momot, P.W. Kuchel, *Concepts Magn. Reson. Part A* 28A (2006) 249-269.
- [4] G. Pages, C. Delaurent, S. Caldarelli, *Anal Chem.* 78 (2006) 561-566.
- [5] G. Pages, C. Delaurent, S. Caldarelli, *Angew. Chem. Int. Ed.* 45 (2006) 5950-5953.
- [6] E.O. Stejskal, J.E. Tanner, *J. Chem. Phys.* 42 (1965) 288-292.
- [7] K.F. Morris, C.S. Johnson Jr, *J. Am. Chem. Soc.* 114 (1992) 3139.
- [8] P. Stilbs, *Prog. Nucl. Magn. Reson. Spectrosc.* 19 (1987) 1-45.
- [9] C.S. Johnson, *Prog. Nucl. Magn. Reson. Spectrosc.* 34 (1999) 203-256.
- [10] A. Dehner, H. Kessler, *ChemBioChem* 6 (2005) 1550-1565.
- [11] K.J. Packer, *Mol. Phys.* 17 (1969) 355 - 368.
- [12] M.D. Hurlimann, *J. Magn. Reson.* 184 (2007) 114-129.
- [13] S. Peled, C.-H. Tseng, A.A. Sodickson, R.W. Mair, R.L. Walsworth, D.G. Cory, *J. Magn. Reson.* 140 (1999) 320-324.
- [14] D.H. Wu, A.D. Chen, C.S. Johnson, *J. Magn. Reson. A* 115 (1995) 260-264.
- [15] G. Bodenhausen, R. Freeman, D.L. Turner, *J. Magn. Reson.* 27 (1977) 511-514.
- [16] M.D. Pelta, G.A. Morris, M.J. Stchedroff, S.J. Hammond, *Magn. Reson. Chem.* 40 (2002) S147-S152.
- [17] L. Li, C.H. Sotak, *J. Magn. Reson.* 92 (1991) 411-420.
- [18] S.S. Velan, N. Chandrakumar, *J. Magn. Reson. A* 123 (1996) 122-125.
- [19] P. Vangelder, A. Olson, C.T.W. Moonen, *J. Magn. Reson. A* 103 (1993) 105-108.
- [20] J.P. Stamps, B. Ottink, J.M. Visser, J.P.M. van Duynhoven, R. Hulst, *J. Magn. Reson.* 151 (2001) 28-31.
- [21] R. Kaptein, K. Dijkstra, C.E. Tarr, *J. Magn. Reson.* 24 (1976) 295-300.
- [22] C. Buckley, K.G. Hollingsworth, A.J. Sederman, D.J. Holland, M.L. Johns, L.F. Gladden, *J. Magn. Reson.* 161 (2003) 112-117.
- [23] I.J. Lowe, R.E. Wysoyng, *J. Magn. Reson. B* 101 (1993) 106-109.
- [24] S.J. Doran, M. Decorps, *J. Magn. Reson. A* 117 (1995) 311-316.
- [25] G. Bodenhausen, R. Freeman, G.A. Morris, *J. Magn. Reson.* 23 (1976) 171-175.
- [26] G.A. Morris, R. Freeman, *J. Magn. Reson.* 29 (1978) 433-462.
- [27] Y.-Q. Song, X. Tang, *J. Magn. Reson.* 170 (2004) 136-148.
- [28] P.T. Callaghan, *Principles of Nuclear Magnetic Microscopy*, Oxford University Press, Oxford, 1993.
- [29] A. Sodickson, D.G. Cory, *Prog. Nucl. Magn. Reson. Spectrosc.* 33 (1998) 77-108.
- [30] R.J. Nelson, Y. Maguire, D.F. Caputo, G. Leu, Y. Kang, M. Pravia, D. Tuch, Y.S. Weinstein, D.G. Cory, *Concepts Magn. Reson.* 10 (1998) 331-341.
- [31] H. Ong, C.-L. Chin, S.L. Wehrli, X. Tang, F.W. Wehrli, *J. Magn. Reson.* 173 (2005) 153-159.

- [32] H. Cho, L. Chavez, E.E. Sigmund, D.P. Madio, Y.Q. Song, *J. Magn. Reson.* 180 (2006) 18-28.
- [33] Y.-Q. Song, U.M. Scheven, *J. Magn. Reson.* 172 (2005) 31-35.
- [34] X.P. Tang, E.E. Sigmund, Y.Q. Song, *J. Am. Chem. Soc.* 126 (2004) 16336-16337.
- [35] W. Richter, S. Lee, W.S. Warren, Q. He, *Science* 267 (1995) 654-657.
- [36] J.W. Barros, J.C. Gore, D.F. Gochberg, *J. Magn. Reson.* 178 (2006) 166-169.
- [37] C.J. Turner, *Prog. Nucl. Magn. Reson. Spectrosc.* 16 (1984) 311-370.
- [38] J.W. Barros, D.F. Gochberg, *Chem. Phys. Lett.* 431 (2006) 174-178.
- [39] I. Ardelean, E. Kossel, R. Kimmich, *J. Chem. Phys.* 114 (2001) 8520-8529.
- [40] C. Ramanathan, R. Bowtell, *J. Chem. Phys.* 114 (2001) 10854-10859.
- [41] M. Engelsberg, W.J. Barros, *J. Chem. Phys.* 122 (2005) 0345011-0345014.
- [42] G. Deville, M. Bernier, J. Delrieux, *Phys. Rev. B* 19 (1979) 5666-5688.
- [43] N.M. Loening, J. Keeler, G.A. Morris, *J. Magn. Reson.* 153 (2001) 103-112.
- [44] M.J. Thrippleton, N.M. Loening, J. Keeler, *Magn. Reson. Chem.* 41 (2003) 441-447.
- [45] K.I. Momot, P.W. Kuchel, *J. Magn. Reson.* 169 (2004) 92-101.
- [46] P.W. Kuchel, A. Coy, P. Stilbs, *Magn. Reson. Med.* 37 (1997) 637-643.
- [47] P.W. Kuchel, B.E. Chapman, N. Muller, W.A. Bubb, D.J. Philp, A.M. Torres, *J. Magn. Reson.* 180 (2006) 256-265.
- [48] C. Naumann, W.A. Bubb, B.E. Chapman, P.W. Kuchel, *J. Am. Chem. Soc.* 129 (2007) 5340-5341.